JOURNAL OF GEOPHYSICAL RESEARCH, VOL. 100, NO. A2, PAGES 1779–1792, FEBRUARY 1, 1995

Simulation study of the role of ion kinetics in low-frequency wave train evolution

Bernard J. Vasquez

Space Science Center, Institute for the Study of Earth, Oceans, and Space, University of New Hampshire, Durham

Abstract. The evolution of uniform, parallel propagating, low-frequency ($\lesssim$ion cyclotron) wave trains is followed with a one-dimensional hybrid numerical code with fluid electrons and particle ions. We show that moderate amplitude ($\delta B/B < 1/2$) wave trains give instabilities and saturated states which differ completely from pure fluid evolution. This is most clearly seen when $\beta > 1$ and instability exists for wavenumbers both below and above the wavenumber of an initial, left-handed wave train or pump wave. For corresponding parameters a fluid theory gives only a narrow range of instability above the pump wavenumber where decay and beat instabilities can occur. In simulations wave energy inverse cascades to smaller wavenumbers and into a greater number of forward than backward going waves. In fluids energy by decay goes mostly to backward ones of smaller wavenumber, and energy by beat goes mostly to forward ones of larger wavenumber. Neither fluid instability explains simulation results. The instability is saturated by thermalizing ions and sometimes exciting small wavenumber electrostatic or acoustic modes. In contrast, saturation in fluids first occurs by generating the harmonics of the growing linear modes. Harmonic generation is mostly absent in simulations. Simulations are carried out to long times and mostly reach a limit beyond which no further significant evolution can occur. Application to Alfvénic fluctuations in the solar wind is discussed.

1. Introduction

Infinite wave train solutions of the ideal two-fluid equations can have an arbitrary and constant magnetic intensity or amplitude (B) when propagating parallel to the background magnetic field $\mathbf{B}_o$. There are two circularly polarized wave modes denoted as right-handed (R) with the electron sense of polarization (also called a fast mode) and left-handed (L) with the ion sense (also called an Alfvén mode). Each has a constant wavenumber k_o and wavefrequency ω_o. For long wavelengths they correspond to the nondispersive magnetohydrodynamic (MHD) modes.

These wave trains or pump waves are in equilibrium, but they can be destabilized by an infinitesimal compressional or sound wave. This has been shown in a number of studies [e.g., *Terasawa et al.*, 1986; *Wong and Goldstein*, 1986; *Hollweg*, 1994] by linearizing the one-dimensional (1-D) two-fluid equations with perturbations of density and longitudinal ion velocity given by $\exp(-i(kx - \omega t))$, where $k(c/\omega_{pi})^{-1}$ is the wavenumber normalized to the ion inertial length c/ω_{pi}, $\omega\Omega_i$ is the wave frequency normalized to ion gyrofrequency Ω_i, xc/ω_{pi} is the distance in the direction of $\mathbf{B}_o$, and $t\Omega_i^{-1}$ is the time. In these equations a term corresponding to the ponderomotive force of the pump wave gives rise to solutions which differ from the incompressible and infinite wave train solutions which occur in the absence of a pump. A solution to the linear equations can be constructed in terms of electromagnetic sideband waves at $k_o + k$ and $\omega_o + \omega$ (upper sideband) and at $k_o - k$ and $\omega_o - \omega$ (lower sideband). Thus we have a three-wave interaction, excluding the pump. These sideband waves always have the same polarization sense as the pump. An important criterion is the propagation direction of the sideband waves, either forward (f) in the direction of the pump or backward (b). A subscript is added to this notation so that $+(-)$ indicates the upper (lower) sideband and s signifies a sound wave; ω as a function of k can be determined as an eigenvalue of the linearized equations. When ω is complex, the pump wave is unstable and grows exponentially at a rate given by the imaginary part of ω. Typically, instabilities occur over a range of k and have one k where the growth rate maximizes.

Pump wave instabilities are very sensitive functions of mode type, B (normalized to B_o), and plasma $\beta(= 8\pi P/B_o^2$, where P is the total plasma pressure). (Note this definition of β differs from the one sometimes used in linear analysis of the instabilities, where it is defined as the ratio v_s^2/v_A^2 with v_s as sound speed and v_A as Alfvén speed. This ratio can be roughly taken as one half the value of β used in this paper.) *Jayanti and*

Paper number 94JA02724.
0148-0227/95/94JA-02724$05.00

Hollweg [1993b] have devised a set of approximate formulae giving the growth rate as a function of β and B for nondispersive waves. *Hollweg* [1994] has given a graphical summary of this behavior for weak dispersion. The nature of the instabilities can be discussed in terms of several types which can occur alone or in combinations. These can be identified by the interaction of eigenmodes of the linearized two-fluid equations in the limit of $B = 0$, where a two-wave interaction predominates, with the third wave carrying relatively little energy when $B^2 \ll 1$.

An unstable sound wave perturbation with $k < k_o$ gives rise to a modulational instability, so-called because the total magnetic intensity, which varies in phase with the sound wave, changes magnitude on a length scale greater than the wavelength of the pump or carrier wave and so modulates it. It is principally due to the interaction of a f_- and f_+ wave. The unstable range of k is generally broad and extends to $k = 0$. The L (R) mode is unstable for $\beta \lesssim (\gtrsim) 2$ and only for sufficiently small B. The instability exists only in the presence of ion wave dispersion and so does not occur in the nondispersive MHD fluid. Another instability at $k < k_o$ has been recently identified by *Hollweg* [1994]. This involves an interaction between f_- and f_s, occurs only in a narrow range of $\beta \approx 1$, and does not include $k = 0$ in its unstable range.

For $k > k_o$, two distinct instabilities are known. Decay instability involves a f_s and b_- wave. For $\beta < 2$, pump waves of either mode are unstable by decay. *Jayanti and Hollweg* [1993b] have shown that the wavenumber of maximum growth varies as $k/k_o = 2/(1 + (\beta/2)^{1/2})$ where $k \ll 1$. Beat instability occurs near $k \approx k_o$ and has f_+ and b_- interaction. Energy predominately goes to the forward going, upper sideband wave in contrast to decay, where energy most often resides in the backward going lower sideband. In most studies, decay overshadows beat, but *Hollweg* [1994] has pointed out that for $\beta > 2$, the beat instability can be the only one which a wave train undergoes.

Numerical fluid simulations by *Hoshino and Goldstein* [1989] have shown that wave train instabilities occur over the linearly predicted range of k. Unstable wave modes grow at the expense of the pump. Of the order of several linear growth times, the pump is shown to steepen (disintegrate) when the instability occurs at $k < (>) k_o$, and sideband waves begin to replace the pump. The linear phase is saturated through nonlinear wave interactions. Hoshino and Goldstein have outlined a weakly nonlinear theory for higher-order mode coupling which they have validated with simulations. To the next order beyond linear, the self-interaction of unstable modes excites nth order harmonics. The dispersion function $D(\omega, k)$ for linear waves can be shown to be of the same form for the higher-order couplings, and so eigenvalues of $D(n\omega, nk)$ are n times those of the linear eigenvalues. Thus the second harmonic can grow twice as fast as the fundamental, the third harmonic 3 times as fast, and so on. This creates a cascade of energy up to large k/k_o, slowing and eventually halting the exponential growth of the fundamental and linear mode. Furthermore, a mean longitudinal velocity flow results from the generated linear sound wave. Hoshino and Goldstein have argued that this is important for giving a turbulent spectrum, since energy is simultaneously transferred to modes of both small and large k/k_o.

Even if the initial wave train were incoherent, evolution akin to these fluid instabilities can still occur. *Umeki and Terasawa* [1992] have shown with a MHD simulation that for small β, incoherent wave trains evolve as if subjected to a decay instability.

The evolution of a wave train has been used as an idealized model of the evolution of Alfvénic fluctuations observed in the solar wind. These fluctuations have been observed whereever spacecraft have sampled [e.g., *Belcher and Davis*, 1971; *Roberts and Goldstein*, 1991]. They mostly propagate outward from the Sun and have large amplitudes, nearly constant field strength, and very low frequencies. Their properties show evidence of turbulence [e.g., *Coleman*, 1968; *Burlaga and Turner*, 1976], and certainly they are not uniform wave trains. As determined from power spectra, these fluctuations evolve with increasing distance from the Sun [e.g., *Denskat and Neubauer*, 1982; *Bavassano et al.*, 1982; *Luttrell and Richter*, 1988]. For instance, the rugged invariant cross helicity [e.g., *Marsch and Mangeney*, 1987] is not conserved and instead decreases with heliocentric distance [e.g., *Matthaeus and Goldstein*, 1982; *Roberts et al.*, 1987a, b; *Tu et al.*, 1989]. Power residing in inward (or sunward) propagating wave modes increases with distance. Observations also show that compressional fluctuations can be coupled to Alfvenic fluctuations. *Grappin et al.* [1990] reveal that the daily turbulent energies in outward and inward magnetic power vary as a function of local sound speed and density fluctuation amplitude $\delta n/n$. *Marsch and Tu* [1990] show that the amplitude of compressional fluctuations increases as high-speed streams radially expand, and it has been further noted by *Roberts et al.* [1987a, b] and *Luttrell and Richter* [1988] that the amount of Alfvenic fluctuations decreases with heliocentric distance. One possible explanation is that a spectral transfer of energy is occurring that produces inward propagating waves in larger amounts as the Alfvenic fluctuations travel further from the Sun. This can be likened to the decay instability of a uniform L mode wave train, which gives backward going waves, and such a process could be one contributor to inward waves. An alternative explanation is that the inward waves are produced by an incompressible instability due the shearing of streams [e.g., *Roberts et al.*, 1992], but *Klein et al.* [1993] have argued from observations that the compressional component can play a large role in the turbulence even if shearing is absent.

From fluid calculations, growth rates of this decay, which are approximately proportional to the pump wave frequency, are very small, and the linear growth time is at least several days and possibly more than the convection time from the Sun to the Earth [e.g., *Cohen and Dewar*, 1974]. Thus to describe this transfer, rates must be calculated for plasma conditions both near and

far from the Sun. Near the Sun, β is small, and a fluid description can suffice. However, near 1 AU, β is of the order of unity, and ion (T_i) and electron (T_e) temperatures are comparable. Thus wave-particle effects should be considered for a complete understanding of these processes.

The influence of ion kinetics can be approached via simulation or linear analysis. Electrons are treated as a massless, quasi-neutral fluid under the assumption that their kinetic effects are unimportant at low frequencies where the displacement current can be neglected. *Terasawa et al.* [1986] used a 1-D hybrid simulation to investigate wave train instabilities. Several runs were made for mostly the R mode at B between 0.5 and 1 and $\beta = 0.3$ and 0.6 with $T_i = T_e$. The initial wave train had $k_o = 0.408$. With this relatively large wavenumber, growth times are $\sim 10\Omega_i^{-1}$, and simulations can follow evolution over many such growth times. (For 1 AU, $c/\omega_{pi} \approx 10^2$ km, so that wavelengths of $\sim 10^3$ km were examined by Terasawa et al., whereas Alfvenic fluctuations have average wavelengths of $\sim 10^6$ km.) For the sake of clarity, we introduce the terminology type M for instability at $k < k_o$ and type D at $k > k_o$, so that fluid instabilities will not be confused with kinetic ones. Terasawa et al. observed only type D instability, in agreement with the decay instability expected from a corresponding fluid. Growth rates were reduced by no more than 30% from the linear fluid rate. This instability was then concluded to differ only quantitatively from that of a fluid. They introduced the paradigm of a damped oscillator to account for Landau damping and modified the linearized fluid equations with additional damping terms. According to the calculations they show (see their Figure 5), this gave a reduced growth rate and a slight increase of the range of unstable k with a distinct maximum located at nearly the same k as had occurred without damping.

As the instability proceeded, large-amplitude density fluctuations were created, ions became trapped, and then they rapidly thermalized. Wave energy was lost to ions, and the instability was saturated. Wave power appeared predominately in backward going modes corresponding to the unstable sidebands expected from the linearized fluid equations. They gave strong emphasis to the success of linear fluid calculations. Further evolution showed a continual transfer of wave energy to smaller wavenumbers with slow ion heating.

Inhester [1990] has examined the linear instability of wave trains, using the drift kinetic and Maxwell's equations. As such the treatment is limited to $k_o \ll 1$, and so neglects dispersion, which excludes a type M instability, but it is applicable to the very long wavelength fluctuations observed in the solar wind. Detailed results were presented for the L mode with $B = 0.44$ at all β. For all T_i/T_e, type D instability occurs, but at large β its character at $T_i/T_e \gtrsim 1$ departs greatly from the fluid one (at $T_i/T_e = 0$) where the unstable range of k is greatly increased with no distinct maximum. The maximum growth rate here differs by no more than 70% from the corresponding fluid rate. The instability appears to be qualitatively different from the fluid one. Although a detailed treatment of the nature of the instability is not given, Inhester has suggested that wave-particle effects give rise to a negative energy wave, as occurs for many plamsa instabilities [e.g., *Hasagawa*, 1975; *Melrose*, 1986]. The energy of this wave is the amount needed to bring it from zero amplitude to some finite value. Though a positive energy wave may be damped, such as a sound wave, a negative energy wave, if present, actually gains the energy lost by this damping. Alternatively, just the existence of a dissipative medium may provide the source of energy to be gained by a negative energy wave. Thus collisionless dissipation can bring on whole new ranges of unstable k in a manner differing completely from that in an ideal fluid. Formally, such an instability is called resistive, while the instability in an ideal fluid is called reactive [e.g., *Craik*, 1985].

Comparing the conclusions of *Inhester* [1990] with those of *Terasawa et al.* [1986], we find two very different views on the role of ion kinetics. Terasawa et al. said that kinetics mostly modify instabilities by just slowing their growth rates, whereas Inhester shows that kinetics can give instability over ranges of k with no correspondence to the pure fluid instability. In an attempt to reconcile these views, Inhester proposed that rapid changes in ion temperatures make simulation results incomparable to his linear analysis. However, we have verified from simulations that the ion temperatures hardly change in the linear phase of the instability, and most ion heating occurs only when the instability saturates. Simulations and linear analyses should give comparable results during the early stages of an instability. Thus Inhester's proposal is not correct, and a real discrepancy between these views remains to be resolved.

Further insight into the role of ion kinetics can be gained from studies of very weakly modulated wave trains. *Mjølhus and Wyller* [1986, 1988] used guiding center equations for ions and derive an evolutionary equation for $B^2 \ll 1$ and $k < 1$. This equation is related to the fluid derivative nonlinear Schrödinger (DNLS) equation [e.g., *Mio et al.*, 1976; *Dawson and Fontán*, 1988] but is valid for all β and accounts for wave-particle effects. It also excludes the type D instability. Mjølhus and Wyller showed that the density δn and B^2 are correlated in a manner distinct from a fluid when $\beta \gtrsim 1$ and $T_i \gtrsim T_e$. Furthermore, a type M instability occurs for both senses of polarization, all k, and most $\beta > 0$ when $T_i \gtrsim T_e$. In fluids, modulational instability varies very differently with these parameters. An analysis with Vlasov equations by *Spangler* [1989, 1990] gave similar results. *Vasquez and Cargill* [1993] have shown with simulations that when $T_i \gtrsim T_e$ the correlation between δn and B^2 in moderate amplitude wave packets is the one anticipated by the above studies. No simulation study has been made to confirm the existence of their type M instability.

In this paper we reconsider the simulation approach to study wave train instabilities and evolution. Again we take $k_o = 0.408$ to facilitate comparison with *Terasawa et al.* [1986], but this study is conducted over a large-parameter space, including $\beta > 1$ and $B < 0.5$,

and giving equal emphasis to R and L modes. We will try to reconcile linear analysis with simulations in hopes of determining the actual role of ion kinetics in wave train evolution.

The outline of this paper is as follows. Section 2 explains the simulation method and initial conditions, and section 3 presents the simulation results. Section 4 gives our conclusions, and section 5 discusses applications and further work.

2. Simulation Method and Initial Conditions

In our simulations, ions are time advanced with an explicit second-order accurate Runge-Kutta scheme, and moments are computed with a second-order weighting scheme. Periodic boundaries are used, and ions upon crossing a boundary are reinjected at the other end, from which it follows that the total number of ions remains constant. Fields are explicitly time advanced, and derivatives are computed from a fast Fourier transform (i.e., a pseudo-spectral method is used).

The algorithm was constructed independently but is based on the one described by *Terasawa et al.* [1986]. The resulting hybrid code has been successfully benchmarked on a variety of problems. Fluidlike behavior can occur when $T_i/T_e \approx 0$. Linear wave trains ($B \ll 1$) propagate with constant wave energy. The simulation results of *Hoshino and Goldstein* [1989] are recovered. We find the same wave train instabilities (both modulational and decay) and unstable k range for their R and L mode wave trains with $k_o = 0.2$, $B = 0.5$, and $\beta = 0.2$ and 2. Furthermore, harmonic generation in the weakly nonlinear phase is also recovered from our hybrid simulations. Kinetic behavior can occur when $T_i/T_e = 1$. In such cases, we can fully reproduce the evolution of the R mode with $B = 1$ and $\beta = 0.55$ shown by *Terasawa et al.* [1986]. We can also reproduce the hybrid simulation results of *Machida et al.* [1987], who examined the evolution of initially modulated wave trains with a maximum amplitude of 0.5.

Our simulations are initialized with a uniform wave train which has either sense of polarization and an arbitrary amplitude. With $k_o = 0.408$, the L (R) mode has $\omega_o = 0.33\,(0.5)$. (For simplicity, k_o and ω_o are always taken to be nonnegative and so do not indicate propagation direction or wave helicity.) The transverse wave velocity is chosen to be parallel to the transverse magnetic field so that the wave travels antiparallel to B_o and in the $-x$ direction. In figures, the initial wave train will move to the left. Waves traveling to the left will be said to move forward. Typically, we include 8 complete cycles of this wave train in the simulation box and use 256 simulation cells. Therefore the total box length is 123 and the cell size Δx is 0.48. In this periodic box, fields are represented by a Fourier series of integral wave modes. The initial wave is mode ± 8 where the $+(-)$ sign is for the L (R) mode, while other wave modes differ from neighboring ones by $\Delta k = k_o/8 = 0.05$. Decreasing Δx gives better spatial resolution, but in terms of Fourier modes it does not change Δk and instead gives only more modes at higher k. Δk can only be decreased and resolution improved by starting with more wave cycles in the simulation box. Typically, a time step $\Delta t = 0.05$ (in units of inverse proton gyrocycles) is employed. Several simulations with smaller Δx, Δk, and Δt have been made, and these give similar results.

Typically, 100 ion particles per cell are used. Similar results are obtained if 400 particles and the highly accurate cubic spline fitting [e.g., *Tajima*, 1989] are used to determine moments. Ions are initially distributed according to the prescription of an isotropic Maxwellian with $T_{i\perp} = T_{i\parallel}$, where $T_{i\perp}$ ($T_{i\parallel}$) is the ion temperature perpendicular (parallel) to the direction of wave propagation. This initial distribution is not a solution of the Vlasov equations, and within a wave period these ions relax to a state with $T_{i\perp}/T_{i\parallel} > (<) 1$ for the L (R) mode. They then remain in this state, which we conclude to be a true equilibrium, until a wave train instability progresses significantly. Such anisotropic ion distributions can indeed be in equilibrium with the wave train and are not neccessarily accessible sources of free energy. *Abraham-Shrauner and Feldman* [1977] give steady, nondispersive, and nonlinear wave train solutions for Vlasov and Maxwell equations which have anisotropic ion distributions. Furthermore, if the anisotropic distributions did undergo instability, this would cause wave growth and would increase the amount of wave energy above its initial value. This energy increase is not seen in simulations.

The ratios of the specific heat of ions γ_i and electrons γ_e are important to the fluid wave train instabilities because these depend on v_s^2/v_A^2, which is proportional to a ratio of specific heat. In simulations, the electrons are treated as a fluid with a pressure which varies as n^{γ_e}, where n is the electron charge density (which is equal to that of the ions). Here we take γ_e to be 1, which corresponds to an isothermal fluid. The γ_i is not a chosen parameter in a hybrid simulation. Its effective value can be determined by making a scatterplot of the logarithm of ion pressure versus the logarithm of density from each simulation cell at some time when the density has departed from its background value n_o. From such plots it has been determined that a straight line fit approximates the distribution with reasonable accuracy and on average has a slope corresponding to $\gamma_i = 1.3$, which is between an isothermal and adiabatic exponent. If ion pressure perpendicular and parallel to the direction of propagation is separately determined, the exponents often differ, which shows that ion behavior need not resemble a simple fluid. However, for our purposes, it will be sufficient to use $\gamma_i = 1.3$ when comparing simulation results with a pure fluid.

To compare with a pure fluid, we first normalize the temperature of each species to $B_o^2/8\pi n_o$, so that its dimensionless value corresponds to the plasma β per species. Then, simulations with a total $\beta (= T_e + T_i)$ are comparable to a pure fluid if β is replaced by $(\gamma_e T_e + \gamma_i T_i)/2$.

Our simulation code accurately conserves total en-

ergy, which is the sum of the magnetic and ion kinetic energy density. (Electric energy density is not considered because we have neglected the displacement current in the simulations.) With our typical choice of parameters, energy is conserved to within 3% at $t = 1500$ and at 30,000 time steps. It tends to increase linearly with time due to a truncation error. This error gives an energy increase because ions tend to walk randomly through erroneous fields and so are stochastically heated [e.g., *Hockney and Eastwood*, 1989].

Terasawa et al. [1986] claimed that the isothermal nature of the electrons meant that energy conservation could not be guaranteed and by implication that energy conservation is not a clear indicator of performance. However, we find that electrons in no way determine energy conservation because they are massless and they have no kinetic energy. This can be checked for cases with $\gamma_e \neq 1$, where an internal electron energy can be defined [e.g., *Jeffrey*, 1966]. This internal energy depends on n. Since the total number of particles in the simulation is a time constant, the sum of n over all cells is also constant, and hence this internal energy is conserved, independent of all else.

As the initial wave train evolves, the transverse magnetic and ion energy densities oscillate, but their sum remains constant. *Terasawa et al.* [1986] reported this and sought to interpret it as a kinetic effect which occurred because the wave train is not initially in a true equilibrium when $T_i/T_e \neq 0$. Moreover, they noted that test particle ions do not conserve energy and oscillate in value. However, we find that the oscillations occur when $T_i/T_e = 0$, so that ion kinetics cannot explain them. Also, test particle behavior gives the general motion of individual particles in the wave field, but hybrid simulations are self-consistent and conserve energy. With time, ion temperatures readjust and reach equilibrium, but the oscillations persist.

We have instead concluded that the oscillations result from a purely numerical effect related to a particle's finite size from which its contribution to the total velocity in a particular cell is determined. We know that the particle size must matter because oscillations vanished for $T_i/T_e = 0$ when the weighting function of each particle was reduced to a δ function, so that it has no size, and moments were collected by using a spectral procedure. (Note that a finite particle size is absolutely necessary when the ions are warm because particle size is used as proxy for the ion probability density, and so a δ function cannot often be used.) On the basis of simulations and analysis, we propose that when the ion transverse velocity moment is determined from particles with a finite size, it does not generally lie exactly in the direction of the transverse magnetic field as it should in an infinite wave train of constant amplitude, and so it is numerically in error. In our code this causes the wave amplitude to vary with time. However, the effect is numerically stable because as the transverse velocity overshoots to one side of the transverse magnetic field, subsequent evolution causes it to return and overshoot to the other side. This oscillation in direction is accompanied by an oscillation in energy density. In the cases presented in this paper, the magnitude of this oscillation is only a few percent or less in energy and can be reduced further by using a smaller Δx, since this gives a more accurate determination of the ion velocity moment. These oscillations appear to have no harmful effect on the physics because the variation of amplitude is essentially across the entire wave train and has a wavenumber of zero, which cannot drive an instability.

Wave steepening as from a type M instability can result in poorly determined derivatives from Fourier analysis and so lead to inaccurate results. This difficulty is well detected by examining the total energy as a function of time. When a portion of the wave is too steep to be accurately represented by a Fourier series, the total energy tends to decrease and then increase back to its expected value as the steepened portion spreads out. Hence one should look for a dip in the curve of energy with time. If a problem exists, then the spatial resolution must be increased. All the simulations reported here have essentially monotonically increasing total energy.

3. Simulation Results

A variational study of the evolution of R and L modes for $B \geq 0.3$ and $\beta \leq 5$ is presented. Evolution from the initial equilibrium is due to linear instabilities. Section 3.1 describes this phase of evolution. Outside of equilibrium (i.e., when the pump wave has lost a few percent of its initial energy), section 3.2 discusses the dynamics of wave-particle and wave-wave interactions which saturate the instabilities and lead to further evolution. Section 3.3 gives the outcome of this evolution at long times.

3.1. Linear Evolution

Fluid instabilities vary intricately over the parameter space and possess threshold amplitudes and β values. *Terasawa et al.* [1986] concluded that the kinetic instability seen in their simulations was a close match to the fluid instability, but they did not examine whether or not it varied with parameters in the same manner as the fluid instability does. Here we first consider a straightforward test. We examine whether or not fluid instability correctly gives instability with respect to k_o, either type M or type D. If the pure fluid proves strongly inconsistent with simulation results, then the kinetic instability must differ fundamentally from that of a fluid. The converse is not true because this test is not very stringent. Where the two are consistent, then they may be closely related, but it is not guaranteed, and one should further consider the detailed behavior as a function of k.

First, consider the L mode. For $B = 0.3$, fluid wave train instabilities have a critical β dependence. For $\beta < 1.4$, modulational instability grows fastest, but decay and beat also occur. For $\beta > 1.4$, only beat occurs. For $\beta < 1.4$, simulations with $T_i/T_e \gtrsim 0.1$ show both type M and type D instabilities. Type M instabil-

ity dominates the other as modulational dominates the others in a pure fluid. However, the kinetic instabilities persist on both sides of k_o above $\beta = 1.4$, so that no critical β dependence exists.

Figures 1a and 1b give the evolution for $\beta = 1.5$ and $T_i/T_e = 0.5$ where pure fluid theory gives only beat instability in a narrow band of wavenumbers (near $m = 10$) resulting in mostly f_+ waves. Figure 1a is a time sequence plot (at intervals of $60\Omega_i^{-1}$) of B (solid line), B_y (dash-dotted line), and B_z (dashed line) as a function of x and t. Evolution is shown from $t = 0$ to 300 through the linear phase and the beginning of the dynamic one. Figure 1b is a plot at $t = 300$ of the wave power in the magnetic field (solid line) and density (dashed line) as a function of m. The pump wave has $m = 8$.

Figure 1a shows that equilibrium is maintained until $t = 180$, after which B varies noticeably with x because instability by this time has resulted in sideband waves with a few percent of the pump wave's initial power. At $t = 240$ and 300, the pump wave is clearly modulated with approximately 4 cycles and steepens in the direction of propagation because wave speed increases with amplitude in the modulated regions, causing larger amplitude regions to overrun smaller ones, as occurs in a shocklet. No right-handed waves result from the steepening. For parallel propagating waves, *Vasquez* [1993] shows that only strongly modulated and large-amplitude wave packets give both steepening and right-handed wave train formation. At $t = 300$ the maximum amplitude occurs near $x = 92$, where $B = 0.5$ and $n = 1.2$.

Figure 1b shows that most of the magnetic wave power resides between $m = 3$ and $m = 5$, corresponding to f_- waves. Density wave power also peaks there. These are all properties of the type M instability. Less magnetic power sits at $m < 0$, and less density power at $m > 8$, showing that the type D instability is relatively weak. For $\beta = 2$ and 5, simulations show that the type M instability gives an increasing amount of f_- to b_- wave power with β. In a pure fluid, modulational instability should not even exist for these parameters, let alone be the dominate instability. No reasonable choice of γ_i will reconcile pure fluids and simulations because for large β we would need $\gamma_i < 0$. Yet this type M instability, which exists at all β, is in agreement with the one predicted by *Mjølhus and Wyller* [1986, 1988]. Introducing damping terms into the linearized fluid equations according to the prescription given by *Terasawa et al.* [1986] also gives a broad range of instability for k both below and above k_o. However, the growth rates are smaller by as much as an order of magnitude from those seen in simulations.

For $B \lesssim 0.8$, type M instability remains dominant. For $B \approx 0.8$, type D instability grows at the same rate as type M, and for larger B it dominates. In a pure fluid, modulational instability occurs only below $B \approx 0.8$, with only decay and beat occurring above. For large amplitudes, fluid and kinetic instabilities would seem to correspond. Yet even here a difference is found. For $B = 1$ and $\beta = 5$ the beat instability occurs and leads to mostly f_+ waves. Simulations with $T_i/T_e \gtrsim 1$ give a type D instability but mostly b_- waves. This preference for the lower sideband is widely observed in simulations. No obvious counterpart to the beat instability is seen when $T_i/T_e \gtrsim 1$.

We now turn to the evolution of the R mode. In a pure fluid it also has a critical β dependence and undergoes decay (modulational) instability for $\beta \lesssim (\gtrsim) 3$. Simulations with $T_i/T_e \sim 1$ show a more complex be-

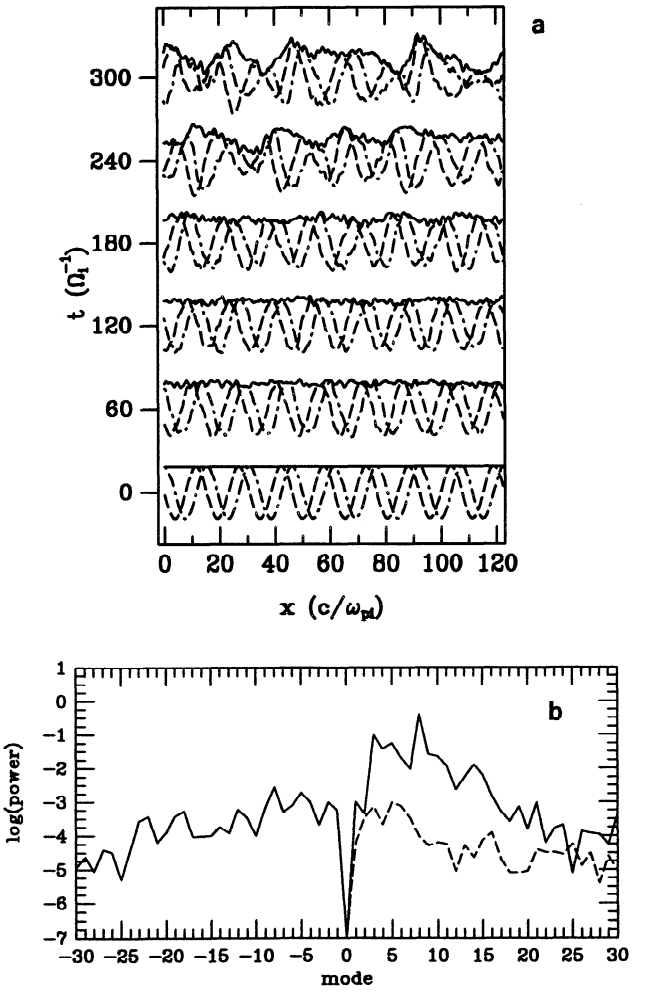

Figure 1. Evolution of the L mode for $B = 0.3$, $\beta = 1.5$, and $T_i/T_e = 0.5$ is shown (a) by a time sequence plot of B (solid line), B_y (dash-dotted line), and B_z (dashed line) as a function of x and t and (b) by a power spectrum for the transverse magnetic field (solid line) and density (dashed line) as a function of mode number at a single time ($t = 300$). The magnetic power is obtained from the square of the Fourier power of $B_y + iB_z$ from which the sign of the mode number corresponds to a helicity. This power is normalized to the initial magnetic power of the pump wave. The Fourier power of density (normalized to the the background density) corresponds to the square of the amplitude of a density mode fluctuation. Since the density is a pure real number, its Fourier transform does not distinguish any helicity, and so it is plotted over only positive mode numbers and would appear the same if also given over negative ones.

havior. Figures 2a and 2b give the evolution of the R mode for $B = 0.5$, $\beta = 5$, and $T_i/T_e = 1.5$, where only modulational instability would occur in a pure fluid. Figure 2a is a time sequence plot of B, B_y, and B_z as a function of x and t. Figure 2b is a plot of the magnetic and density wave power at $t = 300$. The pump wave has $m = -8$.

At $t = 300$ and $x \approx 100$, Figure 2a shows that the pump wave amplitude varies on a shorter length scale than B_y and B_z, which is indicative of type D instability. Figure 2b shows that a large amount of power resides in density at $m = 13$ and 15 and in magnetic at $m = 5$ and 7, corresponding to b_- waves. Nearly equal magnetic power is seen at $m = -4$ corresponding to f_+ waves from a type M instability. Here the instabilities are equally strong. At larger B, and at almost all β, type D dominates. Type M instability dominates only for $B < 0.5$ and $\beta \gtrsim 5$. Hence R mode wave trains undergo a significant type D instability over a larger range than they would in a pure fluid.

Growth rates are an important quantity characterizing any instability. These are measured from simulation quantities by plotting the logarithm of wave power per mode as a function of time. In the linear phase this power tends to grow exponentially and so appears as a straight line on such a plot. The slope of this line is proportional to the growth rate. It is important to note that simulations and linear mode calculations differ in a fundamental way and do not generally give exactly the same growth rates. Simulations solve an initial value problem, and growth rates are determined once the growing mode acquires a significant amount of energy and grows monotonically with respect to the background noise level. From a noise level of $(\delta n)^2 \approx 10^{-4}$ per mode, a growing mode's growth rate is easily measured after increasing by a factor of 10 or more in power and should correspond closely to the rate one would find through an exact solution of the relevant dispersion relation. However, in simulations, modes weakly interact with one another through nonlinearity, and the measured growth rates are skewed from the true linear value. In the fluid limit of $T_i/T_e \approx 0$, simulation growth rates can differ by $\pm 50\%$ from the linear one. This is not a numerical defect of hybrid codes. Fluid simulations show the same behavior when they start from a similar noise level. For instance, the growth rate as determined from a growing mode shown by *Hoshino and Goldstein* [1989, Figure 3] is 28% smaller than the linear rate. Simulations do recover the same linearly unstable range of k but not the same growth rates.

Simulation growth rates are influenced by the number of modes treated and other simulation parameters, since those have influence on the solution of a particular initial value problem. A kind of systematic error between simulation measurements of the growth rate and the true linear one will always exist. Thus a meaningful set of growth rates as a function of T_i/T_e ought to be determined with constant simulation parameters, and the rate at $T_i/T_e \approx 0$ should be used in place of the calculated linear rate. *Terasawa et al.* [1986] should not have used the calculated linear rate to compare with their results at $T_i/T_e = 1$. The trend which emerges from these measurements will be more significant than the individual values of growth rates.

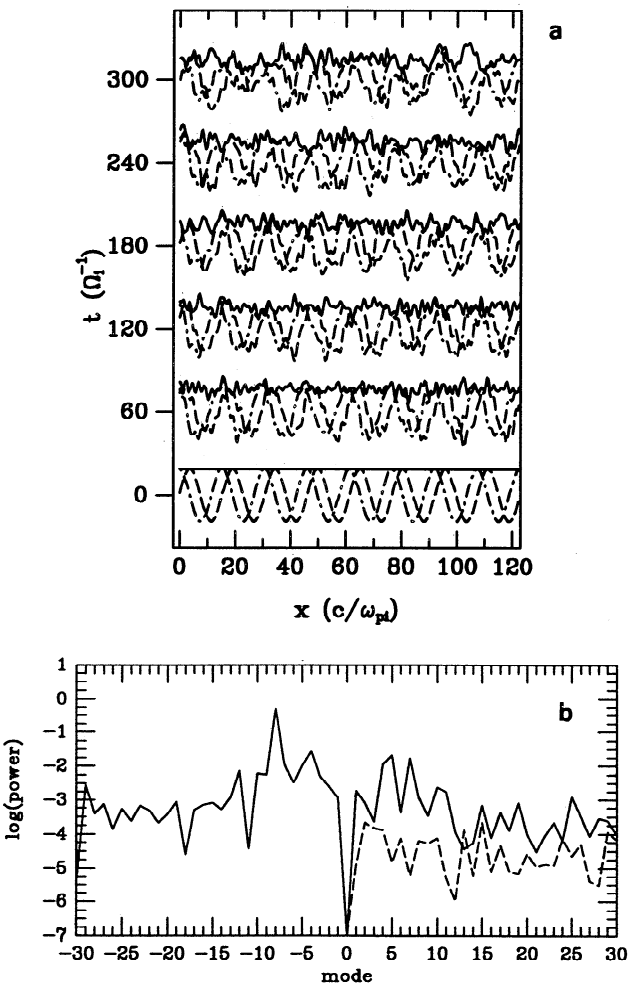

Figure 2. Plots similar to Figure 1 show the evolution of the R mode for $B = 0.5$, $\beta = 5.0$ and $T_i/T_e = 1.5$.

The type D instability for small β is of particular interest to examine in detail. *Terasawa et al.* [1986] saw it as a damped decay, while *Inhester* [1990] saw it as a qualitatively different instability. One approach to this issue is to see how ion kinetics influences its growth rate. Table 1 lists the measured rates in column 3 for the fastest growing density mode of the R mode for $B = 0.5$ and $\beta = 0.45$ as a function of T_i and T_e. For $T_i \approx 0$ the growth rate is approximately 10% of the pump frequency and is 20% smaller than the calculated fluid linear rate. We use this measured value as the fluid rate, and in column 4 we compare all other rates to this one by the percentage of difference. Mode $m = 13$ is the fastest growing mode for $T_i \approx 0$ and is also the fastest one obtained from a linear calculation. For larger T_i the rates decrease as expected for a resistive instability. The total change is no more than 50%, and growth rates for $T_i/T_e \to \infty$ remain within an order of magnitude of the fluid rate. The smallest rate occurs for $T_i = 0.45$, where mode $m = 16$ rather than $m = 13$ grows faster.

Table 1. Maximum Growth Rates of Instability for the R Mode With $B = 0.5$ and $\beta = 0.45$

T_i	T_e	Rate[a]	Difference[b]
0.01	0.44	0.072	...
0.12	0.33	0.062	-14
0.225	0.225	0.053	-26
0.33	0.12	0.043	-40
0.45	0.00	0.040	-44

[a]In Ω_i.
[b]In %.

The unstable range of k is wider for larger T_i, and the growth rate maximizes at a different k. These results are generally consistent with Inhester's portrayal of the type D instability. (A quantitative comparison with his results is not possible because his calculations are valid only for $k_o \ll 1$.) This shows that a sophisticated linear analysis is needed to calculate growth rates in detail. The damped oscillator approach of *Terasawa et al.* [1986] has limited applicability and does not recover these variations with T_i/T_e.

Some simplifications are available if one wishes only to know the properties of instabilities to within an order of magnitude. On average the rate is $\sim 0.1\omega_o B$ for $T_i \approx 0$ and small β, and it decreases by no more than one half as $T_i/T_e \to \infty$. The rate can decrease by another third going from small to large β. The unstable range of k for $T_i/T_c \gtrsim 1$ is typically as broad as the pump wavenumber.

3.2. Dynamic Evolution

At times when the pump wave disintegrates to the point of vanishing, will the emergent wave train match the one corresponding to the sideband of greatest energy calculated by linear theory? *Terasawa et al.* [1986] concluded they did correspond even though these times were well beyond the formal limits of validity of linear theory. Evidence for this was cited from the evolution of the R mode with $B = 1$, $\beta = 0.55$, and $T_i/T_e = 1$. This wave train started out at $m = -8$ (minus sign in accord with our conventions) and underwent a type D instability they said was centered on density mode $m = 12$, which gave the most power to sideband $m = 4$. When the pump wave had vanished, sideband $m = 4$ had the most power, so they concluded linear theory works up to this point.

We find evidence contrary to Terasawa et al.'s conclusion in this matter and can also show that their interpretation of the particular case cited above is inaccurate. First, when other parameters are considered, clear differences were found. For instance, the same R mode as above but with $\beta = 0.37$ undergoes a type D instability, but here the density mode $m = 16$ grew fastest, and so most of the power went to sideband $m = 8$. However, by the time the pump had vanished ($\approx$7 linear growth times later), the emergent sideband of greatest energy was $m = 4$. The discrepancy is due to the manner in which modes are saturated. Though $m = 8$ gains the most power, it saturates early on while the pump still has 50% of its power, at which time the mode $m = 8$ lacks sufficient power relative to the pump to be evident in a plot of the magnetic fields as a function of x. Other modes for $m < 8$ continue to grow and saturate at later times. When the pump finally vanishes, the emergent sideband of greatest energy is not the direct product of the instability but rather has been modified several times through successive inverse cascades. Second, reexamination of the results for $\beta = 0.55$ shows that linear theory using $1 < \gamma_i < 5/3$ actually predicts a maximum growth rate between modes 13 and 14 leading to sideband $m = 5$ or $m = 6$. Mode 13 and not 12 actually grows first in their simulation [see *Terasawa et al.*, 1986, Figure 12b], and so successive cascading has also occurred in this case at times much sooner than noted by Terasawa et al. (see saturation of sideband 5 in their Figure 7). Thus linear theory is unreliable beyond times exceeding a linear growth time. Although linear theory is inapplicable, simulation results for most parameters and $T_i/T_e \gtrsim 1$ show that the sideband of greatest energy after the linear phase will tend to reside at $|m| \lesssim 4$.

Wave-particle interactions are an important saturation mechanism when $T_i/T_e \gtrsim 0.1$. Figures 3a and 3b plot $T_{i\|}$ (solid line) and $T_{i\perp}$ (dashed line) as a function of t from $t = 0$ to 1500. Figure 3a presents these for the R mode with $B = 0.5$, $\beta = 0.45$, $T_i = 0.45$, and $T_e = 0$. This case was also considered in row 5 of Table 1. Figure 3b shows these for the L mode with $B = 0.3$, $\beta = 1.5$, and $T_i/T_e = 0.5$, whose wave evolution is shown in Figure 1. Temperatures first readjust within a pump wave period as discussed in section 2. This is most obvious in Figure 3b, where $T_{i\perp}$ exceeds $T_{i\|}$. When the instability has progressed significantly, the temperatures abruptly rise at $t \approx 60(300)$ in Figure 3a (Figure 3b). The strongest change is in $T_{i\|}$. $T_{i\perp}$ changes simultaneously with $T_{i\|}$ but to a far lesser extent. *Terasawa et al.* [1986] reported a time lag in these changes based on ion thermal energies, which are directly related to temperatures. However, we believe that this is a misinterpretation because they did not realize that the temperature readjusts initially in the wave train to establish a true equilibrium (see section 2). Temperatures grow more slowly after saturation, and for the the R (L) mode shown in Figures 3a and 3b, $T_{i\perp}/T_{i\|}$ approaches 0.5 (0.85). In other cases, this ratio at sat-

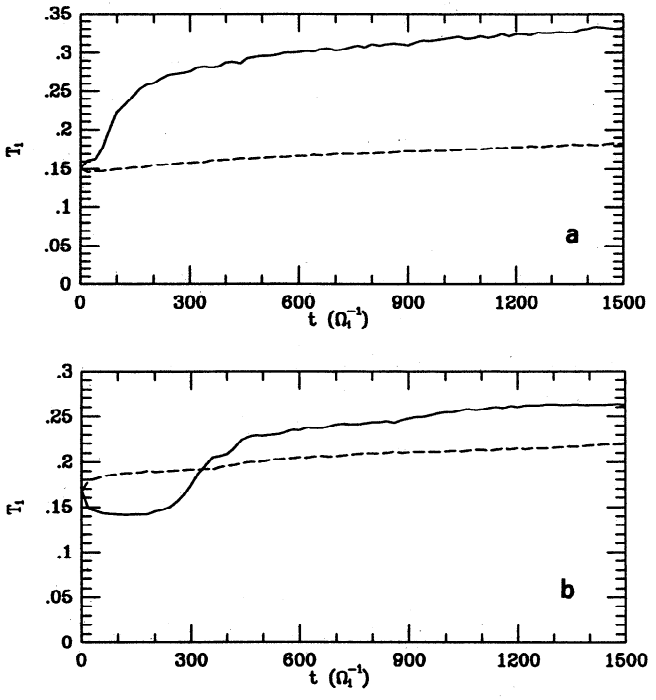

Figure 3. Time history of $T_{i\|}$ (solid line) and $T_{i\perp}$ (dashed line) for (a) the R mode with $B = 0.5$, $\beta = 0.45$, and $T_i/T_e \to \infty$ and (b) the L mode with $B = 0.3$, $\beta = 1.5$, and $T_i/T_e = 0.5$. The dimensionless temperature given here can be expressed in units of electron volts by multiplying it by $2.49B_o^2/n_o$ where B_o is given in units of 10^{-9} T and n_o in units of cm^{-3}.

uration can take different values. Most of this variation can be understood by noting that the larger value of the initial amplitude and the smaller value of T_i or β, then the longer it takes for ions to saturate the instability. Thus $T_{i\|}$ increases more in relation to the value of $T_{i\perp}$, which the wave train had taken when it relaxed into equilibrium. The L mode tends to have $T_{i\perp}/T_{i\|} \sim 1$ at saturation because in equilibrium $T_{i\perp} > T_{i\|}$, whereas the R mode tends to have $T_{i\perp}/T_{i\|} < 1$ because this inequality is met at equilibrium and even more so when $T_{i\|}$ increases at saturation.

The most important force acting on ions is due to the electric field in the direction of wave propagation, which results partly from the forces proportional to the variation in x of the electron pressure and B^2. When $B \gtrsim 0.5$, the amplitude of the electric field or potential is often large enough to reflect ions and thermalize them strongly. This reflection has been observed by tracing individual particles in simulations. Typically, the slower initial bulk population of ions has guiding centers which drift slowly in x until reflected and trapped by the large potentials of a growing compressional wave component. A few reflections increase the drift speeds of these ions until they finally escape. This reflection process was noted by *Terasawa et al.* [1986]. Another important process occurs simultaneously with reflection for large B or alone at small B; this is a form of Landau damping involving nonresonant ions and possibly resonant ones. The strong increase of $T_{i\|}$ seen in simulations is consistent with this form of damping. *Terasawa et al.* [1986] also concluded similarly. This damping affects any compressional component generated from an instability and is most significant when $T_i/T_e \gtrsim 0.1$, as is true for ion acoustic waves in general.

Ion cyclotron damping occurs for particles with speed $V_R = (1 - \omega_o)/k_o$ in the direction of wave propagation. For $k_o = 0.408$, $V_R = 3.7\,(1.6)$ for the R (L) mode. There are very few ions at these velocities in the simulations, and so little energy is dissipated in this manner.

Wave-particle interactions are evidently the most important factor determining wave evolution in the dynamic phase, because spectral transfer takes place in a manner completely different from that in a pure fluid, where only wave-wave interactions cause saturation. Figures 4a and 4b show the power of the most unstable density mode and its second harmonic as a function of t for the R mode treated in Table 1. Figure 4a gives results for $T_i/T_e \approx 0$ (modes 13 and 26), and Figure 4b for $T_i/T_e \to \infty$ (modes 16 and 32). Based on the weakly nonlinear fluid theory given by *Hoshino and Goldstein* [1989], harmonics of the linearly unstable modes should be generated with greater growth rates than the fundamental. Figure 4a shows that the power in both modes oscillates at early times but then grows because of instability and becomes more monotonic toward $t = 80$. Here, $m = 26$ grows faster than $m = 13$ as expected in this fluid limit. Also (but not shown), the third harmonic is similarly excited, and so are the harmonics of other unstable modes. However, Figure 4b shows that as $m = 16$ steadies with time, $m = 32$ actually decreases slightly and continues to oscillate and does not

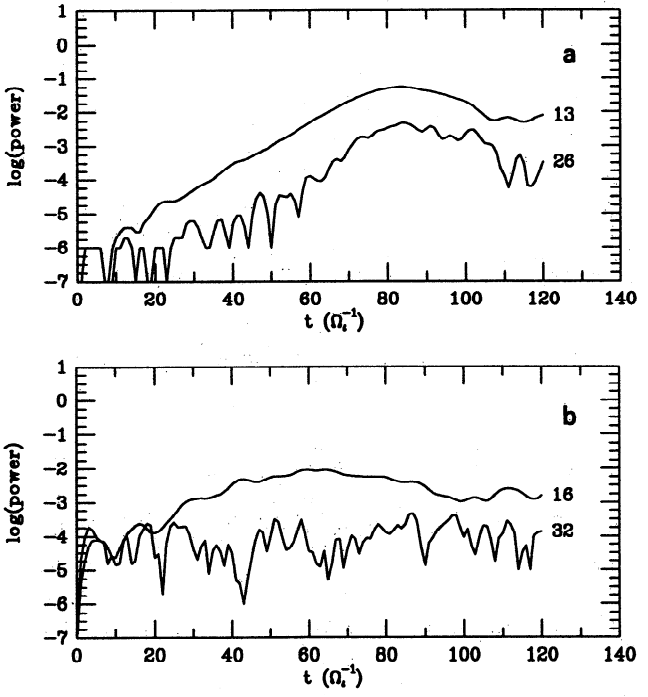

Figure 4. Time history of the wave power for the most unstable density mode and its second harmonic for the R mode with $B = 0.5$, $\beta = 0.45$, and (a) $T_i/T_e \approx 0$ and (b) $T_i/T_e \to \infty$.

grow. The absence of harmonic generation is widely seen in simulations with $\beta \gtrsim 0.5$ and $T_i/T_e \gtrsim 1$. Harmonics are sometimes generated at smaller β even when $T_i = T_e$, showing that wave-wave interactions are not always completely dominated by wave-particle interactions.

Since the density harmonics are not growing, magnetic wave power does not cascade upward in k as much as it does in a pure fluid. Instead, spectral transfer in simulations tends to continue placing more power in the lower sidebands of the linear instability. In some cases where only a type D instability occurs, we have noted a tendency for density modes $m \leq 4$ (smaller than the pump's mode number) to grow just after the wave train passes out of equilibrium. At present we cannot explain why these modes are excited, as no nonlinear kinetic theory is available.

3.3. Long Time Evolution

Simulations have been advanced to $t = 1500$, which includes some 100 pump wave periods and 8 Alfvénic crossings of the simulation box. Evolution of these numerical solutions cannot correspond indefinitely to the true continuous solutions. At these long times, ion heating has slowed and mostly increases at a rate equaling that from the truncation error. Wave power becomes concentrated in a few modes of small wavenumber where no further resolution in k is provided.

Figures 5a and 5b show the evolution of the L mode considered in Figure 1 and extend the results to $t = 1500$. Figure 5a is a time sequence plot of B, B_y, and B_z as a function of x and t. Figure 5b is a plot of the magnetic and density wave power as a function of m. Figure 5a shows that the value of B decreases greatly as the pump wave disintegrates as a result of the type M instability it has undergone. Most of the initial wave power ($\approx$70%) goes to thermalizing ions. Remaining magnetic wave power resides mostly in forward going waves of mode $m = 2$, as shown in Figure 5b. The ratio of forward to backward going wave power is 10 to 1, which is typical when type M instability dominates. When type D instability dominates, this ratio is reversed.

As a function of wavenumber k, magnetic power spectra at these times are broadbanded and tend to be steep for $|k| < k_o$ and flatter for $|k| > k_o$. In Figure 5b the steep portion of the spectrum has an approximate power law dependence of k^{-4} between $m = 2$ and 8. Increasing the resolution of Δk by including 32 cycles of the initial pump wave in the simulation box also gives broadband spectra at $t = 1500$ but shows a number of small maxima supposed on the broad outline of the spectra given in Figure 5b. These maxima are believed to form through the dispersion of waves and not through nonlinear processes.

At $t \sim 1500$, changes in the overall appearance of the wave train are due to wave dispersion rather than a further inverse cascade of wave power. At most times the remaining wave modes destructively interfere, giving no clear wave forms. Occasionally, they reinforce, producing a packet which later disappears as the modes further disperse. This evolution is not sensibly altered when simulations are extended to $t = 2000$. Therefore we conclude that simulations have mostly reached a limit where further significant evolution can only be pursued with greater resolution at smaller k. Presumably, the inverse cascade would continue if this resolution were provided. However, at these times, nonlinear processes affect wave evolution over only long time scales, since the wave amplitudes are only half of what they were initially. Hence dispersion may dominate the evolution as shown in simulations, but a significant role for nonlinear processes cannot be entirely ruled out. Given sufficient time, the waves will spread out, and dispersion may grow less important, allowing nonlinear processes to modify further evolution significantly.

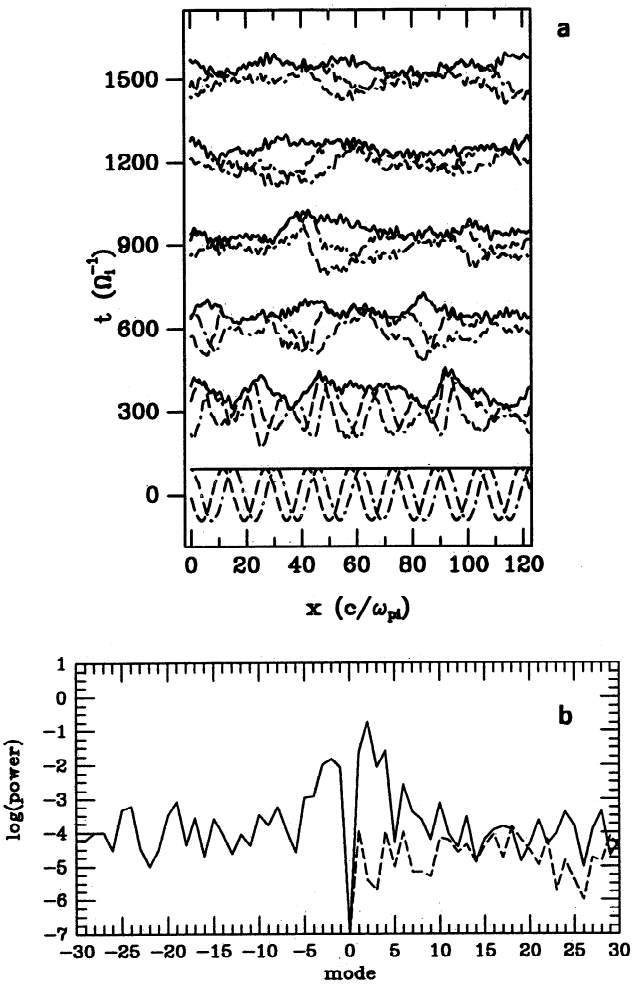

Figure 5. Plots corresponding to Figure 1 show the long time evolution of the L mode for $B = 0.3$, $\beta = 1.5$ and $T_i/T_e = 0.5$.

Evolving pump waves with smaller k_o (such as for Alfvénic fluctuations) or using higher Δk resolution is computationally formidable with a hybrid code. Consider evolving a pump wave with a wavenumber N times smaller than the $k_o = 0.4$, which we have used. Since we must resolve the ion inertial length, the cell size must remain the same. For the simulation box to hold 8 cycles

of this new pump wave, its length will be N times larger and so have N more cells and particles. The computational time is approximately determined by the number of particles to be time advanced, and thus this time will increase by the factor N. Moreover, growth times for instabilities vary approximately as k_o^{-1}, and so we must advance N times further in time than before to reach far into the dynamic phase of evolution. To keep the truncation error to within a few percent, we also need to use a time step which is N times smaller. Hence the required computational time increases as N^3. If we choose $k_o = 0.1$, only a factor of 4 smaller, then it will take 64 times longer for the simulation to be completed in full.

4. Discussion and Conclusions

A 1-D hybrid code with periodic boundaries and a pseudo-spectral field solver is used. Only a discrete set of wavenumbers and hence Fourier modes is numerically representable. The code follows the evolution of a uniform wave train with a constant amplitude B between 0.3 and 1, with either sense of polarization, and with wavenumber $k_o = 0.408$. Plasma β values up to 5 have been considered as well as a range of T_i/T_e. This initial state persists largely unaltered until the growth of unstable modes acquires more than a few percent of the pump wave's initial energy. These instabilities are linear, and log plots of the power per wave mode as a function of time show an approximately constant slope for unstable modes, which is indicative of exponential growth. For $T_i/T_e \approx 0$, unstable wavenumbers match those expected on the basis of linear fluid theory. For $T_i/T_e > 0.1$, ion kinetics becomes a significant factor. In the simplest comparison possible we find that simulation results for $\beta \lesssim 1$ give instability with respect to k_o in the way expected from pure fluids. This parameter range overlaps the one considered by *Terasawa et al.* [1986], who concluded that the type D instability was a just a slower growing version of the decay instability. However, for larger β, pure fluids and simulation results no longer correspond in this sense. For $B \lesssim 0.8$ the L mode undergoes a type M instability at all β, even where it would be modulationally stable in a pure fluid. For $B \gtrsim 0.5$ the R mode undergoes a type D instability for $\beta = 5$ where only modulational instability occurs in a pure fluid. In these cases no reasonable choice of the ion specific heat ratio which determines the sound speed can bring fluid and simulation results into even rudimentary agreement.

Having shown a qualitative difference between fluid and kinetic instabilities, it is clear that at some parameters the instabilities must arise from a very different physics. Yet what about at small β, where they seem to correspond? A careful examination of the instabilities shows that decay and type D instability need not be closely related. For $T_i/T_e > 1$, type D instability tends to exist over a broader range of k and can maximize at a different k from the one seen when $T_i/T_e \approx 0$. Furthermore, growth rates decrease as $T_i/T_e \to \infty$ but by not more than an order of magnitude from the one at $T_i/T_e \approx 0$, and so are never negligible in comparison with fluid instabilities. These conclusions agree with those of *Inhester* [1990].

Ion kinetics appear to play both the role of stabilizer by reducing growth rates and the role of destabilizer by giving instability at completely different ranges of k than in pure fluids. *Terasawa et al.* [1986] essentially missed the importance of the destabilizing role of ion kinetics because their parameter space coverage was too limited to reveal it clearly. Their use of damping terms in linearized pure fluid equations has also been recalculated for the cases treated here. Instability is commonly calculated to exist for k both above and below k_o, as seen in simulations. Instability below k_o is predicted even for their prototype "decay" case of the R mode, although its growth rate is much less than that of the instability above k_o, which may explain why they did not report this. However, a detailed comparison of growth rates shows that the predicted ones can be an order of magnitude smaller than the ones in simulations, especially for $\beta \gtrsim 1$. Therefore the introduction of damping into a pure fluid calculation does not successfully mimic the influence of ion kinetics.

The type M instability of the L mode at $B \lesssim 0.8$ exists at all β and so corresponds to the instability predicted by *Mjølhus and Wyller* [1986, 1988]. In addition, we have shown that above this amplitude it is no longer a significant instability relative to type D instability. Mjølhus and Wyller also predicted that the R mode would undergo type M instability at all β, which is not seen in simulations. Instead, it most often undergoes the type D instability, which is excluded from the kind of analysis carried out by Mjølhus and Wyller. This discrepancy can be resolved if their predicted type M instability grows far more slowly than the type D instability at most parameters.

The L mode with $B = 0.3$ has proven to be the most interesting case presented in this paper and merits greater attention. For $T_i/T_e \gtrsim 1$, power predominately goes to the lower sideband, which proves generally true for all cases where T_i/T_e is large. Power goes into backward (b) and forward (f) going waves in different proportions dependent upon β. Because the type M instability occurs at all β and dominates type D instability, most of the power ($f/b \approx 10$) goes to forward going waves, especially at large β, and shows remarkably modest variation as a function of β. In fluids the beat instability becomes important for large β and produces mostly forward going waves. However, beat causes most of the wave power to go to the upper sideband, which differs from simulation results.

Ultimately, the instability modifies the pump wave, causing it to steepen and then disintegrate when type M instability dominates, or just to disintegrate when type D dominates. The growing modes from the linear phase of evolution are saturated long before the pump wave vanishes. Individual modes saturate at different times. Predicting the outcome of this evolution based on linear theory is not always possible, in contradiction to what

Terasawa et al. [1986] claimed. Saturation is principally caused by the individual motion of ions, which rapidly thermalize once the pump wave has clearly gone out of equilibrium. The ion temperature increases more in the parallel than in the perpendicular direction to propagation. In cases where a large-amplitude electrostatic wave forms, ions become trapped, reflect, and gain energy until they become free. The occurrence of this trapping was first shown by *Terasawa et al.* [1986]. In other cases, a form of ion Landau damping without trapping seems to be the main mechanism.

When wave-particle interactions saturate the instability, an unexpected spectral transfer can result. In fluids, harmonics of the growing linear modes are generated, and they saturate the instability. For $T_i/T_e \gtrsim 1$ and $\beta \gtrsim 1/2$, harmonics tend not grow. Sometimes, compressional modes with wavenumbers smaller than k_o grow instead. Magnetic wave power preferentially goes to smaller wavenumbers, so that an inverse cascade predominates. Just why this occurs is not understood at present, but it clearly shows that wave trains have a nonlinear evolution unlike anything seen in a pure fluid.

Simulations were made over $10^3\Omega_i^{-1}$, which is 10^2 pump wave periods or 8 Alfvén wave crossing times. At these long times, ion heating is mostly indistinguishable from truncation error. Wave modes with small wavenumbers and with different directions of propagation are present. These modes most often destructively interfere, but occasionally reinforce, giving a well-defined but temporary wave packet at some locations. Arguably, simulations have reached their useful limit because significant evolution cannot occur unless Fourier modes with smaller wavenumbers are included in the simulations. Presumably, if the smaller wavenumbers were included, the inverse cascade could continue and might lead to turbulence.

Evolution from an equilibrium could ultimately lead to turbulence, as laboratory experiments of fluid flows have shown [e.g., *Koschmieder*, 1993]. When the energy containing scales and dissipative scales become well separated, a so-called inertial subrange forms at intermediate wavenumbers, where the transfer rates of wave power are essentially independent of dissipation. In this subrange a statistical equilibrium can prevail, so that the transfer rates into and out of each wavenumber are equal and the power spectrum obeys a power law of the form k^{-s}, where s is constant spectral slope. In our case no simulation or analysis of low-frequency waves exists, which convincingly demonstrates that such turbulence will ultimately evolve. Nevertheless, *Hoshino and Goldstein* [1989] suggested from their pure fluid simulations that turbulence would eventually occur if simulations could be pushed far enough. They showed that the nonlinear interaction of modes causes wave power to cascade (e.g., harmonic generation), and at long times their power spectra show many discrete modes at high wavenumbers rather than a continuum. They argued without explicit proof that because additional processes give an inverse cascade, these spectra will ultimately become broadbanded and turbulent. Since there is little dissipation at small wavenumbers in this fluid code, we might also suppose that an inertial subrange will also form where processes giving cascade and inverse cascade come into balance.

Using the same reasoning as above, our simulations with collisionless dissipation do not clearly show any processes which would lead to steady turbulence, since the cascade of wave power is weak in relation to inverse cascade and magnetic power spectra, though already broadbanded, have very steep slopes ($s \sim 4$) for $|k| \lesssim k_o$ at long times. Therefore the occurrence of turbulence with an inertial subrange from wave train evolution is debatable. Only if collisionless dissipation becomes insignificant at smaller wavenumbers, which have not been adequately studied in these simulations, might an inertial subrange form.

5. Applications and Further Work

This study has shown the active role that collisionless dissipation plays in low-frequency wave train evolution. This dissipation is not limited to ion gyroscales because it is a form of Landau damping. This study complements the linear analyses of *Inhester* [1990] and asymptotic studies of *Mjølhus and Wyller* [1986, 1988] and *Spangler* [1989, 1990] which show that Landau damping via resonant particles plays a similar role for even very small pump wavenumbers, which our simulations have not treated. The effect that dissipation can have on instabilities is a fundamental physical phenomenon and is treated in several textbooks [e.g., *Hasegawa*, 1975; *Melrose*, 1986; *Craik*, 1985] which are well worth examining.

Alfvénic fluctuations exist over a continuous range of wavenumbers. They are often treated to lowest order as an incompressible turbulence with energy (e.g., streams) and dissipative (e.g., ion gyroradius) scales so well separated that the fluctuations constituent an inertial subrange. Power spectra tend to have a mean spectral index of 1.7 [e.g., *Bavassano et al.*, 1982; *Tu et al.*, 1989] which is said to be Kolgomorov-like. However, there is now observational evidence (see section 1) to suggest that compressional fluctuations are more important than it would seem from their small ($\delta n/n \lesssim 0.1$) average amplitude. If compressions are important, could the next logical step be to consider the importance of collisionless dissipation at very low frequencies like Landau damping? After all, the solar wind is not a magnetofluid, it is a collisionless plasma, and Alfvénic fluctuations are still considered to be a mesoscale or microscale phenomenon separate from streams and other large-scale structures which are well explained in terms of a pure MHD fluid.

In the solar wind, Landau damping is invoked to explain the relative absence of compressional waves with respect to Alfvénic fluctuations [e.g., *Barnes*, 1979]. Also, it is used in nearly incompressible MHD theory to justify the neglect of acoustic waves as compared to pseudosound [e.g., *Matthaeus et al.*, 1991; *Zank and Matthaeus*, 1992, 1993; *Klein et al.*, 1993]. In each case, Landau damping is used to remove a certain set of wave

modes and then assumed to act passively on all others. However, as we have seen here, collisionless dissipation could actually have an active role, and its presence might alter the spectral transfer. Instead of having Alfvénic fluctuations cascade their power without dissipation until they reach gyroscales, dissipation might occur at all scales, and no inertial subrange would exist. The cascade rate could not then be directly equated to the dissipation rate at ion gyrofrequencies in order to calculate ion heating as *Tu* [1988] has done. Simulations of the Alfvénic fluctuations would have to treat the plasma on an equal footing, since they could be strongly coupled.

Further work should be done to complement this study and existing linear kinetic analyses and to examine the relevance of these wave train studies to Alfvénic fluctuations. First, a linear kinetic analysis with dispersion should be made. This could verify the instabilities seen in simulations and would provide a more complete reporting of growth rates as a function of the parameters. Moreover, one should determine whether or not a negative energy wave mode exists since this could give insight into the nature of the instabilities. V. Jayanti (private communication, 1994) is currently adapting the method of analysis outlined by *Lee and Kaw* [1972], which will ultimately give linearized kinctic equations characterizing wave train instabilities with finite dispersion in the limit of $B^2 \ll 1$. Second, simulations should be carried out at very small k values, which are relevant to Alfvénic fluctuations in the solar wind, to examine the nonlinear stages which *Inhester* [1990] could not address. Hybrid codes which must resolve the ion inertial length are not useful for this purpose. It might be done by using a guiding center code for the particles.

Starting from nonmonochromatic wave trains with properties like those observed for Alfvénic fluctuations, simulations should be performed to determine whether or not warm protons cause evolution to differ from pure fluid evolution. This should help settle the issue raised in this paper concerning the possible significance of kinetics. If kinetics prove important, one should include in simulations the complicated proton distribution functions [e.g., *Marsch et al.*, 1982] actually observed in association with the Alfvénic fluctuations and in high-speed streams. The proton pressure can be determined in simulations and compared to the density fluctuations to see whether or not an equation of state can be deduced which matches the empirical one obtained by *Marsch and Richter* [1987]. In addition, the equation of state can be compared to the ones deduced from a nearly incompressible MHD theory.

The high-speed solar wind also has an important population of streaming α particles having approximately 4% of the proton number density and 16% of the proton thermal pressure [e.g., *Neugebauer*, 1981]. In a pure fluid, *Hollweg et al.* [1993] show that additional wave train instabilities and beam instabilities occur with conditions corresponding to the solar wind. The role of ion kinetics in these instabilities has not yet been explored. Moreover, electrons tend to be 2-3 times hotter than protons, and so their particle nature could also warrant examination.

In nature one must also consider the multidimensional character of wave train evolution, which may not correspond to that in 1-D. For instance, the filamentary instability [*Kuo et al.*, 1988] occurs for perturbations perpendicular to the background magnetic field and is not recovered in the limit of one dimension. Linear analysis in higher dimensions is complicated by the fact that sidebands are infinitely coupled, and a linear solution cannot be constructed with just two [*Jayanti and Hollweg*, 1993a]. Particle simulations have been few [e.g. *Liewer et al.*, 1992; *Viñas and Goldstein*, 1992] and limited to small β. They have demonstrated the existence of both a filamentary and type D instability. As it has been for 1-D simulations, it would seem worthwhile to search the parameter space more completely for two dimensions.

Acknowledgments. This work was supported by the NASA Space Physics Theory Program under grant NAG5-1479 to the University of New Hampshire. We thank Z. Agim, P. Cargill, R. Grappin, J. Hollweg, P. Isenberg, M. Lee, and A. Vinas for helpful discussions and especially V. Jayanti for providing some linear fluid calculations and for the many conversations we have had concerning this work.

The Editor thanks E. Marsch and another referee for their assistance in evaluating this paper.

References

Abraham-Shrauner, B., and W. C. Feldman, Nonlinear Alfvén waves in high-speed wind streams, *J. Geophys. Res.*, *82*, 618, 1977.

Barnes, A., Hydrodynamic waves and turbulence in the solar wind, in *Solar System Plasma Physics*, vol. 1, edited by E. N. Parker, C. F. Kennel, and L. J. Lanzerotti, p. 249, North-Holland, New York, 1979.

Bavassano, B., M. Dobrowolny, F. Mariani, and N. F. Ness, Radial evolution of power spectra of interplanetary Alfvénic turbulence, *J. Geophys. Res.*, *87*, 3617, 1982.

Belcher, J. W., and L. Davis, Large-amplitude Alfvén waves in the interplanetary medium, 2, *J. Geophys. Res.*, *76*, 3534, 1971.

Burlaga, L. F., and J. B. Turner, Microscale 'Alfvén waves' in the solar wind at 1 AU, *J. Geophys. Res.*, *81*, 73, 1976.

Cohen, R. H., and R. L. Dewar, On the backscatter instability of solar wind Alfvén waves, *J. Geophys. Res.*, *79*, 4174, 1974.

Coleman, P. J., Turbulence, viscosity, and dissipation in the solar-wind plasma, *Astrophys. J.*, *153*, 371, 1968.

Craik, A. D. D., *Wave Interactions and Fluid Flows*, Cambridge University Press, New York, 1985.

Dawson, S. P., and C. F. Fontán, Soliton decay of nonlinear Alfvén waves: Numerical studies, *Phys. Fluids*, *31*, 83, 1988.

Denskat, K. U., and F. M. Neubauer, Statistical properties of low-frequency magnetic field fluctuations in the solar wind from 0.29 to 1 AU during solar wind minimum conditions: Helios 1 and 2, *J. Geophys. Res.*, *87*, 2215, 1982.

Grappin, R., A. Mangeney, and E. Marsch, On the origin of solar wind MHD turbulence: Helios data revisited, *J. Geophys. Res.*, *95*, 8197, 1990.

Hasagawa, A., *Plasma Instabilities and Nonlinear Effects*, Springer-Verlag, New York, 1975.

Hockney, R. W., and J. W. Eastwood, *Computer Simulation Using Particles*, Adam Hilger, New York, 1989.

Hollweg, J. V., The beat, modulational and decay instabilities of a circularly-polarized Alfvén wave, *J. Geophys. Res.*, **99, 23,431, 1994.**

Hollweg, J. V., R. Esser, and V. Jayanti, Modulational and decay instabilities of Alfvén waves: Effects of streaming He^{++}, *J. Geophys. Res.*, *98*, 3491, 1993.

Hoshino, M., and M. L. Goldstein, Time evolution from linear to nonlinear stages in magnetohydrodynamic parametric instabilities, *Phys. Fluids B*, *1*, 1405, 1989.

Inhester, B., A drift-kinetic treatment of the parametric decay of large-amplitude waves, *J. Geophys. Res.*, *95*, 10,525, 1990.

Jayanti, V., and J. V. Hollweg, On the dispersion relations for parametric instabilities of parallel-propagating Alfvén waves, *J. Geophys. Res.*, *98*, 13,247, 1993a.

Jayanti, V., and J. V. Hollweg, Parametric instabilities of parallel-propagating Alfvén waves: Some analytical results, *J. Geophys. Res.*, *98*, 19,049, 1993b.

Jeffrey, A., *Magnetohydrodynamics*, Oliver and Boyd, Edinburgh, 1966.

Klein, L., R. Bruno, B. Bavassano, and H. Rosenbauer, Anisotropy and minimum variance of magnetohydrodynamic fluctuations in the inner heliosphere, *J. Geophys. Res.*, *98*, 17,461, 1993.

Koschmieder, E. L., *Bénard Cells and Taylor Vortices*, Cambridge University Press, New York, 1993.

Kuo, S. P., M. H. Whang, and M. C. Lee, Filamentation instability of large-amplitude Alfvén waves, *J. Geophys. Res.*, *93*, 9621, 1988.

Lee, Y. C., and P. K. Kaw, Parametric instabilities of ion cyclotron waves in a plasma, *Phys. Fluids*, *15*, 911, 1972.

Liewer, P. C., T. J. Krücken, R. D. Ferraro, V. K. Decyk, and B. E. Goldstein, Two dimensional pic simulations of plasma heating by dissipation of Alfvén waves, in *Solar Wind Seven*, edited by E. Marsch and R. Schwenn, p. 481, Pergamon, New York, 1992.

Luttrell, A. H., and A. K. Richter, The role of Alfvénic fluctuations in MHD turbulence evolution between 0.3 and 1 AU, Solar Wind Six, vol. 1, *Tech. Note NCAR/TN-306+Proc*, p. 335, Natl. Cent. for Atmos. Res., Boulder, Colo., 1988.

Machida, S., S. R. Spangler, and C. K. Goertz, Simulation of amplitude-modulated circularly polarized Alfvén waves for beta less than one, *J. Geophys. Res.*, *92*, 7413, 1987.

Marsch, E., and A. Mangeney, Ideal MHD equations in terms of compressive Elsässer variables, *J. Geophys. Res.*, *92*, 7363, 1987.

Marsch, E., and A. K. Richter, On the equation of state and collision time for a multicomponent, anisotropic solar wind, *Ann. Geophys.*, *5*, 71, 1987.

Marsch, E., and C.-Y. Tu, Spectral and spatial evolution of compressible turbulence in the inner solar wind, *J. Geophys. Res.*, *95*, 11,945, 1990.

Marsch, E., K.-H. Mühlhäuser, R. Schwenn, H. Rosenbauer, W. Philipp, and F. M. Neubauer, Solar wind protons: Three-dimensional velocity distributions and derived plasma parameters measured between 0.3 and 1 AU, *J. Geophys. Res.*, *87*, 52, 1982.

Matthaeus, W. H., and M. L. Goldstein, Measurement of the rugged invariants of magnetohydrodynamic turbulence in the solar wind, *J. Geophys. Res.*, *87*, 6011, 1982.

Matthaeus, W. H., L. W. Klein, S. Ghosh, and M. R. Brown, Nearly incompressible magnetohydrodynamics, pseudosound, and solar wind fluctuations, *J. Geophys. Res.*, *96*, 5421, 1991.

Melrose, D. B., *Instabilities in Space and Laboratory Plasmas*, Cambridge University Press, New York, 1986.

Mio, K., T. Ogino, K. Minami, and S. Takeda, Modified nonlinear Schrödinger equation for Alfvén waves propagating along the magnetic field in cold plasma, *J. Phys. Soc. Jpn.*, *41*, 265, 1976.

Mjølhus, E., and J. Wyller, Alfvén solitons, *Phys. Scr.*, *33*, 442, 1986.

Mjølhus, E., and J. Wyller, Nonlinear Alfvén waves in a finite-beta plasma, *J. Plasma Phys.*, *40*, 299, 1988.

Neugebauer, M., Observations of solar-wind helium, *Fundam. Cosmic Phys.*, *7*, 131, 1981.

Roberts, D. A., and M. L. Goldstein, Turbulence and waves in the solar wind, *U.S. Natl. Rep. Int. Union of Geod. Geophys. 1987-1990, Rev. Geophys.*, *29*, 932, 1991.

Roberts, D. A., L. W. Klein, M. L. Goldstein, and W. H. Matthaeus, The nature and evolution of magnetohydrodynamic fluctuations in the solar wind: Voyager observations, *J. Geophys. Res.*, *92*, 11,021, 1987a.

Roberts, D. A., M. L. Goldstein, L. W. Klein, and W. H. Matthaeus, Origin and evolution of fluctuations in the solar wind: Helios observations and Helios-Voyager comparisons, *J. Geophys. Res.*, *92*, 12,023, 1987b.

Roberts, D. A., M. L. Goldstein, W. H. Matthaeus, and S. Ghosh, Velocity shear generation of solar wind turbulence, *J. Geophys. Res.*, *97*, 17,115, 1992.

Spangler, S. R., Kinetic effects of Alfvén wave nonlinearity, I, Ponderomotive density fluctuations, *Phys. Fluids B*, *1*, 1738, 1989.

Spangler, S. R., Kinetic effects of Alfvén wave nonlinearity, II, The modified nonlinear wave equation, *Phys. Fluids B*, *2*, 407, 1990.

Tajima, T., *Computational Plasma Physics: With Applications to Fusion and Astrophysics*, Addison-Wesley, Reading, Mass., 1989.

Terasawa T., M. Hoshino, J. Sakai, and T. Hada, Decay instability of finite-amplitude circularly polarized Alfvén waves: A numerical simulation of stimulated brillouin scattering, *J. Geophys. Res.*, *91*, 4171, 1986.

Tu, C.-Y., The damping of interplanetary Alfvénic fluctuations and the heating of the solar wind, *J. Geophys. Res.*, *93*, 7, 1988.

Tu, C.-Y., E. Marsch, and K. M. Thieme, Basic properties of solar wind MHD turbulence near 0.3 AU analyzed by means of Elsässer variables, *J. Geophys. Res.*, *94*, 11,739, 1989.

Umeki, H., and T. Terasawa, Decay instability of incoherent Alfvén waves in the solar wind, *J. Geophys. Res.*, *97*, 3113, 1992.

Vasquez, B. J., Strongly nonlinear evolution of low-frequency wave packets in a dispersive plasma, *Phys. Fluids B*, *5*, 2021, 1993.

Vasquez, B. J., and P. J. Cargill, The evolution of strongly modulated, low-frequency, moderate amplitude wave packets in a dispersive plasma, *Phys. Fluids B*, *5*, 42, 1993.

Viñas, A. F., and M. L. Goldstein, Parametric instabilities of large amplitude Alfvén waves with obliquely propagating sidebands, in *Solar Wind Seven*, edited by E. Marsch and R. Schwenn, p. 577, Pergamon, New York, 1992.

Wong, H. K., and M. L. Goldstein, Parametric instabilities of circularly polarized Alfvén waves including dispersion, *J. Geophys. Res.*, *91*, 5617, 1986.

Zank, G. P., and W. H. Matthaeus, Waves and turbulence in the solar wind, *J. Geophys. Res.*, *97*, 17,189, 1992.

Zank, G. P., and W. H. Matthaeus, Nearly incompressible fluids, II, Magnetohydrodynamics, turbulence, and waves, *Phys. Fluids A*, *5*, 257, 1993.

Bernard J. Vasquez, Space Science Center, Institute for the Study of Earth, Oceans, and Space, University of New Hampshire, Durham, NII 03824.

(Received June 21, 1994; revised October 13, 1994; accepted October 17, 1994.)